Annals of Nuclear Medicine Vol. 17, No. 8, 641–648, 2003

Three-dimensional stereotactic surface projection of brain perfusion SPECT improves diagnosis of Alzheimer's disease

Norinari HONDA,*1 Kikuo MACHIDA,*1 Tohru MATSUMOTO,*2 Hiroshi MATSUDA,*3 Etsuko IMABAYASHI,*3 Jun HASHIMOTO,*4 Makoto HOSONO,*5 Yusuke INOUE,*6 Kiyoshi KOIZUMI,*7 Shigeru KOSUDA,*8 Toshimitsu MOMOSE,*9 Yutaka MORI*10 and Motoo OSHIMA*11

*1*Department of Radiology, Saitama Medical Center, Saitama Medical School*
*2*National Institute of Radiological Sciences*
*3*Department of Radiology, National Center Hospital for Mental, Nervous, and Muscular Disorders*
*4*Department of Radiology, Faculty of Medicine, Keio University*
*5*Department of Radiology, Faculty of Medicine, Kinki University*
*6*Department of Radiology, Institute of Medical Science, University of Tokyo*
*7*Department of Radiology, Tokyo Medical University*
*8*Department of Radiology, National Defense Medical College*
*9*Department of Radiology, Faculty of Medicine, University of Tokyo*
*10*Department of Radiology, Jikei University School of Medicine*
*11*Department of Radiology, Kasukabe Hospital*

Objectives: Alzheimer's disease (AD) is diagnosed by either inspection of the brain perfusion SPECT, or three-dimensional stereotactic surface display (3D-SSP). The purpose was to compare diagnostic performances of these methods. ***Methods:*** Sixteen nuclear medicine physicians independently interpreted ^{99m}Tc-ECD SPECT in one session and SPECT with 3D-SSP in another session without clinical information for 50 studies of AD patients and 40 studies of healthy volunteers. Probabilities of AD were reported according to a subjective scale from 0% (normal) to 100% (definite AD). Receiver operating characteristics curves were generated to calculate areas under the ROC curves (Az's) for the inspection as well as for an automated diagnosis based on a mean Z value in the bilateral posterior cingulate gyri in a 3D-SSP template. ***Results:*** Mean Az for visual interpretation of SPECT alone (0.679 ± 0.058) was significantly smaller than that for visual interpretation of both SPECT and 3D-SSP (0.778 ± 0.060). Az for the automated diagnosis (0.883 ± 0.037) was significantly greater than that for both modes of visual interpretation. ***Conclusions:*** 3D-SSP enhanced performance of the nuclear medicine physicians inspecting SPECT. Performance of the automated diagnosis exceeded that of the physicians inspecting SPECT with and without 3D-SSP.

Key words: brain perfusion SPECT, ROC analysis, Alzheimer's disease, image processing, automated diagnosis

INTRODUCTION

ALZHEIMER'S DISEASE (AD) and other types of dementia can be diagnosed by brain radionuclide tomography by characteristic patterns of perfusion.[1–4] However, diagnosis of AD by visual interpretation of brain perfusion SPECT shows great inter-observer variation,[5] which may decrease the diagnostic effectiveness of SPECT. Statistical manipulation of PET or SPECT images after anatomical standardization, including three-dimensional stereotactic surface projection (3D-SSP)[6–9] and statistical parametric mapping,[10] may eliminate inter-observer variations, and may detect subtle changes indiscernible

Received June 13, 2003, revision accepted September 8, 2003.

For reprint contact: Norinari Honda, M.D., Department of Radiology, Saitama Medical Center, Saitama Medical School, 1981 Tsujido, Kamoda, Kawagoe, Saitama 350–8550, JAPAN.
E-mail: norihnd@saitama-med.ac.jp

by human eyes. Utilization of these methods succeeded in identifying subtle decreases in glucose metabolism[11] or brain perfusion[12,13] in posterior cingulated gyri and precunei in very early AD.

A beneficial effect of additional 3D-SSP on visual interpretation of ^{18}F-FDG PET for diagnosis of AD is reported using receiver operating characteristics (ROC) analysis.[14] However, to our knowledge, such a beneficial effect of 3D-SSP has not been measured for brain perfusion SPECT. Also automated diagnosis of AD through numerical indices derived from 3D-SSP of brain perfusion SPECT is still sparse. The purpose of the present study was to compare performances through ROC analysis between visual interpretation of brain perfusion SPECT with and without 3D-SSP images and an automated diagnosis by 3D-SSP images in diagnosing AD, which included patients in its very early phase.

MATERIALS AND METHODS

Subjects

Materials were 90 studies of ^{99m}Tc-ethyl cysteinate dimer (ECD) brain perfusion SPECT, consisting of 50 studies in 25 patients with AD and 40 studies in 40 healthy volunteers. Each of the patients underwent two SPECT studies separated by a mean of 447 days (range, 328–773).

The patients, 10 men and 15 women with a mean age of 71.2 years (range, 52–84) at the time of the first SPECT, had been followed at an outpatient clinic of memory disorders in the National Center Hospital for Mental, Nervous, and Muscular Disorders. All of the patients presented with minor memory disturbance without signs and symptoms of dementia, and none was diagnosed with AD at the initial presentation. Board-certified psychiatrists of the clinic diagnosed the patients as probable AD during the follow-up based on both DSM-IV and NINCDS-ADRDA criteria[15,16] after exclusion of other diseases by brain MRI. Means of mini-mental state examination (MMSE) score[17] were 26.0 ± 1.46 (range, 24–28) and 22.1 ± 4.42 (range, 14–29) at the time of the first and second SPECT, respectively. In this study, all of the SPECT studies of the patients were deemed to be those of AD even when the clinical diagnosis of AD was not made at the time of SPECT. Precise time from the initial presentation to the clinical diagnosis of AD was not obtainable from the medical records of the patients.

The healthy volunteers were 22 men and 18 women with a mean age of 71.8 years (range, 60–84). Mean MMSE score was 28.2 ± 2.09 (range, 22–30). Written informed consent was obtained before participation. The ethics committee of NCHMNM approved the recruitment of healthy volunteers. The volunteers passed neuropsychiatric examinations, ^{99m}Tc-ECD SPECT, and brain MRI with normal results.

Image generation

Technetium-99m ECD at a dose of 600 MBq was intravenously injected with the patient's eyes closed in a quiet room. Ten minutes after the injection, a three-head SPECT system (Multispect3, Siemens, Malvern, PA, USA), equipped with low-energy, high-resolution, fan-beam collimators, operated in a step-and-shoot mode to collect a set of projection images. The acquisition protocol was 24 projection images arranged at 5-degree intervals for each head, sampling time of 50 seconds at each head position, and 128 × 128 matrices. The image set was processed with a Hanning filter of 0.7 cycle/cm followed by reconstruction of transverse images with Shepp-Logan filtered back projection. Attenuation correction of Chang's method was applied assuming an attenuation coefficient of 0.09/cm. A set of color-coded SPECT images in transverse, sagittal, and coronal planes were printed on a sheet of 28-by-21 cm glossy photo paper (Fig. 1A).

Then, 3D-SSP images were created according to the reports[6–10] on a computer workstation by software licensed from the originators, and printed on a sheet of 28-by-21 cm paper (Fig. 1B). A set of 3D-SSP images was composed of eight projection images of Z values over the brain surface. The Z values were calculated on a pixel-by-pixel basis by the following equation[9] after anatomical standardization[6–8] to compensate for inter-individual variation in brain shape. Z = (mean of normalized pixel value of normal database − normalized pixel value of a patient)/SD of the database. SPECT studies composing the normal database for 3D-SSP were the same as those reported by Kogure et al.[12]

Image interpretation

Sixteen nuclear medicine physicians from eight institutions participated in an image interpretation experiment. Careers in nuclear medicine varied from 1 to 20 years, and two of them were experts in nuclear neurology. The experts were from the data source institution. Self-reported experience with 3D-SSP of brain perfusion SPECT for AD is shown in Table 1. Thirteen of the participants gathered to form two general sessions held 12 weeks apart. Three physicians finished two sessions at their own institutions 4 weeks apart outside the general sessions.

The physicians independently interpreted only SPECT images in the first session, and both SPECT and 3D-SSP images in the second session. They were not informed of the patients' age, gender, or other clinical information except for the fact that the materials comprising normal and AD cases. They also were not informed of the number of the AD cases. The order of inspection in the second session, SPECT first or 3D-SSP first, was left to the participants. The cases were reviewed in the same order in the first and second sessions for each observer.

They reported the probability of AD for each case according to a subjective linear scale ranging from 0% (normal) to 100% (definite AD) in both of the sessions.

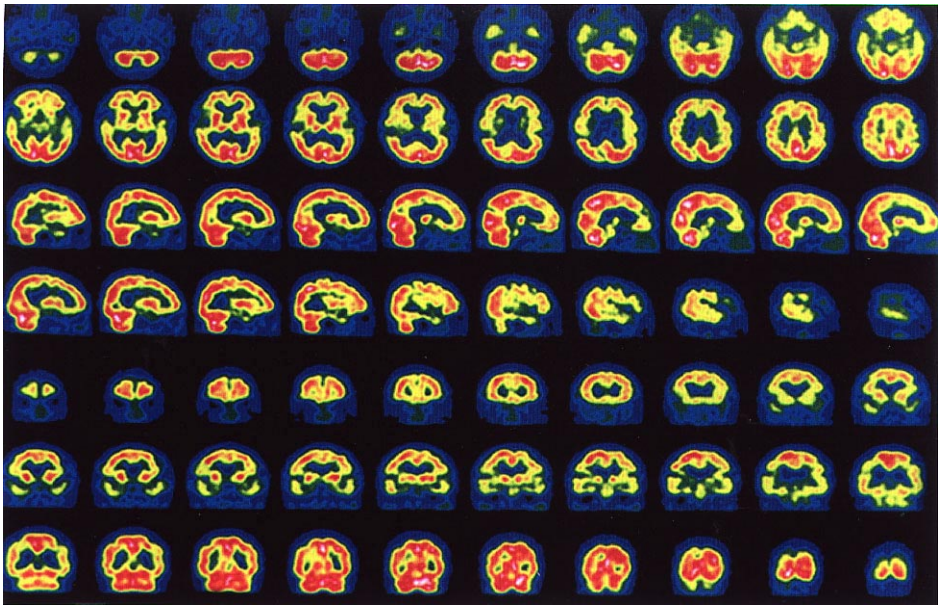

A

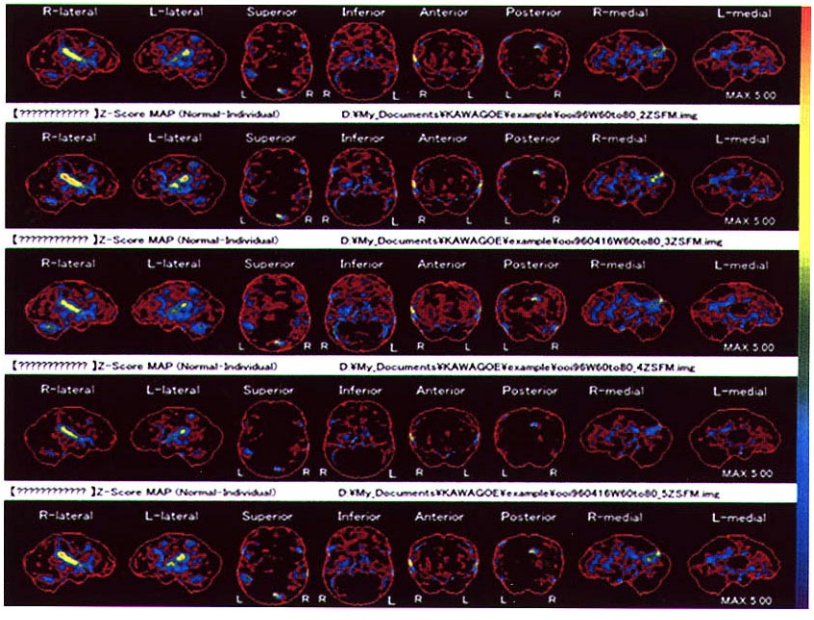

B

Fig. 1 Representative color-coded SPECT images (A) and 3D-SSP images (B) used for the image interpretation experiment. A SPECT image set in A comprised transverse (the first to the second line), sagittal (the third to the fourth line), and coronal images (the fifth to the seventh line). An image set in B comprises images normalized to the thalami in the first line, to the cerebral global mean in the second line, to the cerebellum in the third line, to the pons in the fourth line, and to primary sensory cortex in the fifth line. Images in each line of B are, from left to right, right lateral, left lateral, superior, inferior, anterior, posterior, right mid-sagittal, and left mid-sagittal view.

They were requested not to report a possibility of 50%. Time required for reviewing each case was measured by recording the start and finish time of the interpretation for the case.

At the beginning of the sessions, the participants received lectures, and practiced on one normal SPECT study and four studies of two patients. The studies for practice were not included in the study materials. Allotted time for the lecture and practice was 30 minutes in total. The lecture before the first session explained the typical SPECT findings in AD and diagnostic criteria of SPECT. The criteria were hypoperfusion of bilateral posterior cigulate gyri and precunei in the very early phase,[12,13] additional hypoperfusion in the bilateral medial temporal

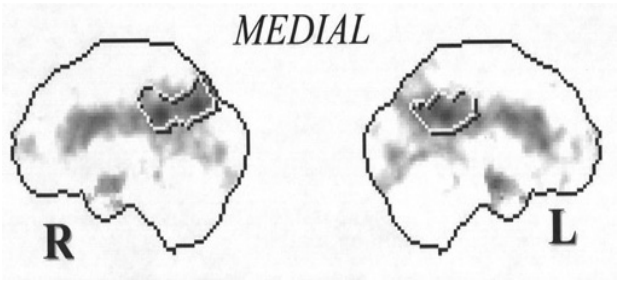

Fig. 2 Regions of interest placed in the right (R) and left (L) posterior cingulated gyri and precunei on the mid-sagittal 3D-SSP templates for the automated diagnosis to calculate a mean Z value. Difference in the ROI shapes was the result of a study by some of the authors (submitted).

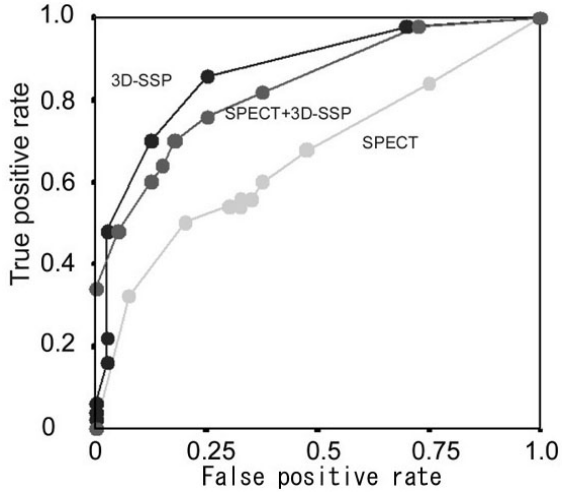

Fig. 3 Representative ROC curves of a physician (Physician C in Table 1) for inspection of SPECT alone (SPECT), inspection of SPECT with 3D-SSP (SPECT + 3D-SSP), and the automated diagnosis (3D-SSP).

lobes in the early phase,[1–5] and bilateral temporoparietal hypoperfusion with or without uni- or bi-lateral frontal hypoperfusion in the advanced phase.[1–5] Perfusion of the sensorimotor cortex, occipital cortex, and cerebellum is not reduced in any of the phases.[4] In the lecture before the second session, they were instructed to rely mostly on the 3D-SSP images normalized to the cerebral global mean among the five sets of the 3D-SSP images for inspection in this experiment.

Data analysis

The diagnostic gold standard in a subsequent analysis was the final diagnosis made by the psychiatrists as described. Receiver operating characteristics (ROC) curves were generated for each observer using a SSP version 10 statistical software package. In the processing, two relative cumulative frequency curves were derived from histograms of the probability given to AD cases and to normal cases by each observer. Data on the two curves at the same probability value yielded true positive rate and false positive rate. By changing the probability, an ROC curve was generated. Probability greater than 50% was deemed as positive diagnosis of AD for an analysis by 2 × 2 contingency table to calculate sensitivity and specificity.

Diagnostic performance was also assessed for an automated diagnosis method. The automated diagnosis was defined as diagnosis solely based on a mean of the Z values in the predefined region of interest (ROI) in the posterior cigulate gyrus and precuneus on 3D-SSP images (Fig. 2) normalized to cerebral global mean. Means of the Z values, i.e. pixel values, in the ROI's on the right and left cerebral hemispheres were calculated separately. Then an average of the two was calculated as a representative Z value for the automated diagnosis. ROC curves were generated in the same way as ROC analysis of the SPECT inspection replacing AD probability with the representative Z values.

Statistical test

Areas under the ROC curves (Az's) were calculated with SPSS statistical software (version 10) according to the Metz method.[18,19] Paired t-test was employed to test differences in interpretation time between the individual physicians and between the inspection modes, as well as to test differences in Az's between the two modes of visual interpretation. The statistical tests for the other indices were noted in the RESULTS section. Probability values less than 5% were deemed significant.

RESULTS

Interpretation time of inspection of SPECT only was longer in 9, same in 3, and shorter in 4 of the 16 observers than that of inspection of both SPECT and 3D-SSP (Table 1). Inspection time differed significantly among the physicians (ANOVA, $p = 0.0009$). But, the mean of interpretation time of the 16 physicians was not significantly changed between inspection of SPECT only and that of SPECT with 3D-SSP (Table 1, $p = 0.30$).

Representative ROC curves of one physician (Physician C in Table 1) are shown in Figure 3. In the case of this physician, Az for visual interpretation of SPECT alone was significantly smaller than that for both SPECT and 3D-SSP ($p < 0.05$), although the greatest Az was obtained by the automated diagnosis. The same trend, the greatest Az for the automated diagnosis followed by visual interpretation of SPECT with 3D-SSP, was observed in all but one of the participating physicians (Table 1). The automated diagnosis yielded a specificity of 70% and sensitivity of 90% using the threshold Z value of 0.384, or specificity of 78% and sensitivity of 80% using the thresh-

Table 1 Comparison of diagnostic performances by ROC analysis and time efficiency

Physician	Area under the ROC curve by the inspection		Time required for the inspection		Change in inspection time by addition of 3D-SSP#	Self-reported experience with 3D-SSP for AD (cases)
	SPECT (Az ± SD)	SPECT with 3D-SSP (Az ± SD)	SPECT (s/case)	SPECT with 3D-SSP (s/case)		
A	0.704 ± 0.054	0.893 ± 0.036*	44	34	S	600
B	0.752 ± 0.051	0.850 ± 0.040	64	54	S	250
C	0.667 ± 0.057	0.833 ± 0.042	80	50	S	0
D	0.657 ± 0.058	0.828 ± 0.043	37	25	S	100
E	0.754 ± 0.052	0.825 ± 0.043	38	35	UC	20
F	0.728 ± 0.054	0.809 ± 0.046	71	48	S	20
G	0.718 ± 0.054	0.802 ± 0.047	65	90	L	0
H	0.648 ± 0.059	0.777 ± 0.048	45	53	L	70
I	0.673 ± 0.058	0.775 ± 0.049	57	48	S	20
J	0.699 ± 0.055	0.763 ± 0.050	33	43	L	0
K	0.607 ± 0.061	0.732 ± 0.052	84	73	S	5
L	0.662 ± 0.057	0.731 ± 0.054	90	95	UC	30
M	0.550 ± 0.062	0.731 ± 0.053	42	62	L	5
N	0.748 ± 0.055	0.729 ± 0.053**	48	33	S	10
O	0.706 ± 0.055	0.715 ± 0.054	57	60	UC	100
P	0.595 ± 0.060	0.659 ± 0.057	42	30	S	50
Mean	0.679	0.778	56	53	—	80
SD	0.058	0.060	17	20	—	148
CV	0.084	0.062	0.31	0.38	—	1.85

Note: Area under the ROC curve (Az) by the automated diagnosis was 0.883 ± 0.037, which was significantly greater (Metz method) than those of SPECT and SPECT with 3D-SSP.

* Az of inspection of SPECT with 3D-SSP exceeded the Az of the automated diagnosis in this physician only.

** Addition of 3D-SSP to SPECT lessened the Az in this physician only.

Results of paired t-test (p = 0.01): S, shortened; UC, unchanged; L, lengthened.

old Z value of 0.506 by the ROC analysis.

Mean Az of the 16 doctors for visual interpretation of SPECT alone (mean ± SD, 0.679 ± 0.058; range, 0.550–0.754) was significantly smaller than that for visual interpretation of both SPECT and 3D-SSP (mean ± SD, 0.778 ± 0.060; range, 0.659–0.893, p = 0.0001). Az for the automated diagnosis (0.883) was significantly greater than the mean Az for both modes of visual interpretation (Metz method,[18,19] $p < 0.05$ for both). Inter-observer variation of diagnostic performances (SD of Az's) was not significantly different between visual interpretations of SPECT and SPECT with 3D-SSP (Levence statistics, p = 0.857, Fig. 4). The automated diagnosis gave the same Az for repeated trials to result in complete reproducibility.

The analysis by 2 × 2 contingency table showed that sensitivity was lower in 9, not changed in 1, and higher in 6 of the 16 participants by the addition of 3D-SSP, while specificity for visual interpretation of both SPECT and 3D-SSP was higher in 12, equal in one, and lower in three doctors of the 16 participants (Table 2). Mean sensitivity did not change (p = 0.457, Wilcoxon signed rank test), but mean specificity increased significantly ($p < 0.016$, Wilcoxon signed rank test) by the addition of 3D-SSP.

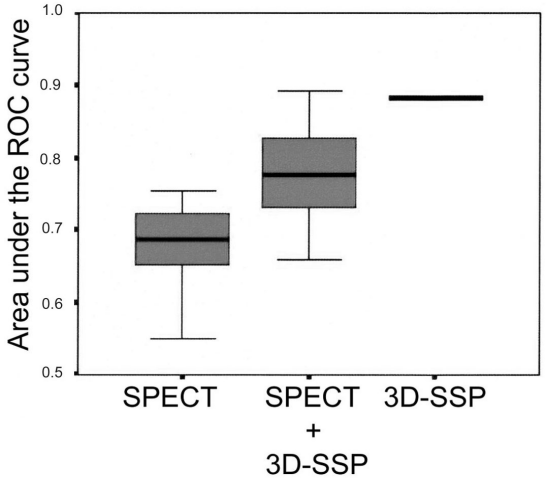

Fig. 4 Distribution of Az's grouped by the modes of diagnosis. Name of the groups is the same as Figure 3. Upper and lower ends of the boxes represent 75 and 25 percentile. Horizontal bars denote means. Variation in Az's was not different between SPECT and SPECT + 3D-SSP.

Table 2 Comparison of diagnostic performances by 2 × 2 contingency table

Physician	Diagnosis by SPECT		Diagnosis by SPECT with 3D-SSP	
	Sensitivity (%)	Specificity (%)	Sensitivity (%)	Specificity (%)
A	76	45	90	72
B	68	70	58	90
C	45	68	64	85
D	72	58	68	87
E	86	47	94	47
F	88	33	94	55
G	58	85	56	92
H	78	50	60	75
I	78	53	70	65
J	78	45	70	75
K	66	58	42	92
L	74	50	66	72
M	88	23	92	12
N	88	55	80	50
O	42	88	76	60
P	52	60	52	62
Mean	71.3	55.5	70.8	68.2
SD	14.5	16.3	15.3	20.3
CV	0.20	0.29	0.22	0.30

Mean sensitivity was not different ($p = 0.457$), while mean specificity was different ($p < 0.016$).

DISCUSSION

We utilized two sets of brain perfusion SPECT for each AD patient. The aim of this design was to ensure a wide range of severity of AD would be available ranging from the pre-clinical stage to clinically detectable stage. Though none of the patients fulfilled the clinical diagnostic criteria of AD at the time of the first SPECT, they were regarded as the cases of AD in this study. Such patients, not meeting NICS-ADRDA criteria but having hypoperfusion in the posterior cingulate gyri, were included as AD in two other studies[13,20] besides this study. Inclusion of very early, or, pre-clinical AD is an important point of the study, which influenced the diagnostic performance of the physicians. We compared diagnostic power of two modes of inspection, SPECT alone and SPECT with 3D-SSP in the present experiment. We did not measure the diagnostic performance of inspection of 3D-SSP images alone. The intervals of 3 to 12 weeks between the two sessions were intended to reduce bias arising from observers' familiarity with the study materials.

This study revealed that addition of 3D-SSP images to SPECT inspection enhanced diagnostic performances of the nuclear medicine physicians in diagnosing AD. Areas under the ROC curve (Table 1) and specificity (Table 2) increased, whereas sensitivity and inter-observer variation did not. One factor accounting for these results may be the inclusion of SPECT of very early AD. Very subtle change made the detection of abnormality difficult resulting in the low sensitivity. The absence of landmarks on 3D-SSP images to identify the posterior cingulated gyri may be another factor. The absence of landmarks may make distinction between image noise and true hypoperfusion difficult, and thus sensitivity was not improved with the addition of 3D-SSP to SPECT inspection. Although there were physicians with very limited experience with 3D-SSP (Table 1), inspection time did not change as a whole, and over half of the physicians shortened their inspection time. Thus we think 3D-SSP is a useful adjunct in the brain perfusion SPECT interpretation.

Improvement of diagnostic accuracy by addition of 3D-SSP images has been reported previously for ^{18}F-FDG brain PET.[14] The performance of the doctors in the present study is worse, with Az of SPECT inspection smaller than 0.9, than that of the doctors in PET inspection.[14] A possible reason for the different diagnostic performances is that image resolution was worse in our SPECT than their PET. Images obtained by lower resolution system are reported to result in smaller Az's than those obtained by higher resolution.[21] Another possible reason is the non-linear relation between flow and accumulation of ^{99m}Tc-ECD. Extraction of ^{99m}Tc-ECD in the brain diminishes at high flow rates,[22] and thus image contrast between areas of reduced and normal flow is lessened making detection of hypoperfusion difficult. In addition, differences in the study population may be, at least in part, responsible for the difference in diagnostic performance.

For the automated diagnosis by 3D-SSP, we chose the average of the two mean Z values of the bilateral posterior cingulate gyri and precunei as the diagnostic criterion. Since reduced glucose metabolism or hypoperfusion in these areas is reported to be present in very mild to moderate AD,[11–13,20] we expected that sensitive diagnosis of AD from its early phase was possible with this criterion. As a result, we attained a specificity of 70% to keep with the specificity of 90% by the threshold Z value of 0.384. This result seems acceptable because half of the AD cases were in its very early phase, in which other diagnostic imaging may be powerless.

Accuracy, i.e. Az, of the automated diagnosis outweighed both types of inspection. Also the automated diagnosis showed much smaller variation in performance, i.e. SD of Az's, than the physicians. This finding may indicate that AD could be diagnosed more reproducibly by the automated method based on 3D-SSP images than by visual inspection. However, this result cannot be generalized, since there is population bias of the study materials and the physicians. Inclusion of pre-clinical AD intuitively makes the inspection difficult (study population bias). Observer population bias is exemplified by the fact that the two nuclear neurology experts in the par-

ticipants (physician A, B in Table 1) were the top two performers. Even if the results could be generalized, physicians can still play important roles in pointing out artifacts arising from inappropriate data handling and presence of areas of hypoperfusion outside the target areas to avoid misdiagnosing as AD.

Other methods of automated diagnosis of AD by PET or SPECT are reported. Neural network approach yielded Az of 0.95 and 0.87 for high resolution and low resolution ^{18}F-FDG PET, respectively, for more advanced AD with a mean MMSE score of about 15[21] than in this study. Posterior cingulate gyrus was not paid particular attention in their study. Attained Az of 0.88 in the present study is similar to Az of low resolution PET,[21] even though our study contained very early AD.

Singular value decomposition was adapted to brain perfusion SPECT obtaining a diagnostic accuracy of 72% for mild AD patients who were before conversion from non-AD to probable AD as categorized by NINCS-ADRDA criteria.[13] The study of Helholtz et al.[20] utilized statistical parametric mapping to sum up t-values of the voxels with their values smaller than 95% of the normal database in the areas where characteristic hypometabolism of FDG was observed. The summed t-value resulted in Az of 0.93 for discriminating very mild AD (MMSE > 24) from normal. The Az value is comparable to the results of this study (Az = 0.883), considering that SPECT was used instead of PET.

In conclusion, 3D-SSP enhanced specificity, but not sensitivity, of SPECT inspection by the nuclear medicine physicians with unchanged interpretation time as well as inter-observer variation in this study. Performance of the automated diagnosis, based on the mean Z value within ROI drawn in the posterior cingulated gyri and precunei, exceeded those of the physicians inspecting SPECT with and without 3D-SSP in this study.

ACKNOWLEDGMENTS

This study was financially supported by a grant from the Japanese Society of Nuclear Medicine, grant for cancer research of Hasegawa from Ministry of Health, Welfare, and Labor of Japan, and grant from the Ministry of Education, Culture, Sports, Science and Technology of Japan (C-10670869). The authors thank the physicians who participated in the image interpretation experiments. The authors thank Takeo Takahashi, MD and Shinya Oku, MD for valuable comments on the manuscript. The authors also thank Nihon Medi-Physics Co., for supporting the meetings of the authors, and Daiichi Radioisotope Laboratories, Co. for renting rooms and office equipment for the experiments.

REFERENCES

1. Read SL, Miller BL, Mena I, Kim R, Itabashi H, Darby A. SPECT in dementia: clinical and pathological correlation. *J Am Geriatr Soc* 1995; 43 (19): 1036–1043.
2. Donnemiller E, Heilmann J, Wenning GK, Berger W, Decristoforo C, Moncayo R, et al. Brain perfusion scintigraphy with ^{99m}Tc-HMPAO or ^{99m}Tc-ECD and ^{123}I-beta-CTT single photon emission tomography in dementia of the Alzheimer-type and diffuse Lewy body disease. *Eur J Nucl Med* 1997; 24: 320–325.
3. Bonte FJ, Weiner MF, Bigio White CL. Brain blood flow in the dementias: SPECT with histopathologic correlation in 54 patients. *Radiology* 1997; 202: 793–797.
4. Matsuda H. Cerebral blood flow and metabolic abnormalities in Alzheimer's disease. *Ann Nucl Med* 2001; 15: 85–92.
5. Honda N, Machida K, Hosono M, Matsumoto T, Matsuda H, Oshima M, et al. Interobserver variation in diagnosis of dementia by brain perfusion SPECT. *Radiation Medicine* 2002; 20: 281–289.
6. Minoshima S, Berger KL, Lee KS, Mintun MA. An automated method for rotational correction and centering of three-dimensional functional brain images. *J Nucl Med* 1992; 33: 1579–1585.
7. Minoshima S, Koeppe RA, Mintun MA, Berger KL, Taylor SF, Frey KA, et al. Automated detection of the intercommissural (AC-PC) line for stereotactic localization of functional brain images. *J Nucl Med* 1993; 34: 322–329.
8. Minoshima S, Koeppe RA, Frey KA, Kuhl DE. Automated standardization: linear scaling and non-linear warping of brain functional images. *J Nucl Med* 1993; 35: 1528–1537.
9. Minoshima S, Frey KA, Koeppe RA, Foster NL, Kuhl DE. A diagnostic approach in Alzheimer's disease using three-dimensional stereotactic surface projections of florine-18-FDG PET. *J Nucl Med* 1995; 36: 1238–1248.
10. Frith CD, Friston KJ, Ashburner J. Principals and methods. In *Human Brain Function*, Frackowiak RSJ, Friston KJ, Frith CD, Dolan RJ, Mazziotta JC (eds), 1st ed, San Diego; Academic Press, 1997: 3–159.
11. Minoshima S, Giordani B, Berent S, et al. Metabolic reduction in the posterior cingulate cortex in very early Alzheimer's diseases. *Ann Neurol* 1997; 42: 85–94.
12. Kogure D, Matsuda H, Ohnishi T, Asada T, Uno M, Kunihiro T, et al. Longitudinal evaluation of Alzheimer's diseases using brain perfusion SPECT. *J Nucl Med* 2000; 41: 1155–1162.
13. Johnson KA, Jones K, Holman BL, Becker JA, Spiers PA, Satlin A, et al. Preclinical prediction of Alzheimer's disease using SPECT. *Neurology* 1998; 50: 1563–1571.
14. Jonathan HB, Minoshima S, Borght TV, Tran DD, Kuhl DE. Alzheimer's disease: Improved visual interpretation of PET images by using three-dimensional stereotactic surface projection. *Radiology* 1996; 198: 837–843.
15. Diagnostic and statistical manual of mental disorders. 4th ed. (DSM-IV). Washington, DC; American Psychiatry Association, 1994: 123–163.
16. McKhann C, Drachman D, Folstein M, Katzman R, Price D, Stadlan EM. Clinical diagnosis of Alzheimer's Disease: report of the NINCDS-ADRDA work group under auspices of Department of Health and Human Services task force on Alzheimer's Disease. *Neurology* 1984; 34: 939–944.
17. Folstein MF, Folstein DE, McHugh PR. "Mini-mental state." A practical method for grading the cognitive state of patients for the clinician. *J Psychiatr Res* 1975; 12: 189–198.
18. Metz CE. ROC methodology in radiology imaging. *Invest*

Radiology 1986; 21: 720–733.
19. Metz CE. Some practical issues of experimental design and data analysis in radiological ROC studies. *Invest Radiol* 1989; 24: 234–245.
20. Herholz K, Salmon E, Perani D, Baron J-C, Holthoff V, Frolich L, et al. Discrimination between Alzheimer Dementia and controls by automated analysis of multicenter FDG PET. *NeuroImage* 2002; 17: 302–316.
21. Kippenhan JS, Barkeer WW, Nagel J, Grady C, Duara R. Neural-network classification of normal and Alzheimer's disease subjects using high-resolution and low-resolution PET. *J Nucl Med* 1994; 35: 7–15.
22. Di Rocco RJ, Silva DA, Kuczynski BL, Narra RK, Ramalingam K, Jurisson S, et al. The single-pass cerebral extraction and capillary permeability-surface area product of several putative cerebral blood flow imaging agents. *J Nucl Med* 1993; 34: 641–648.